Acta Oto-Laryngologica, 2012; Early Online, 1–7

informa
healthcare

CASE REPORT

Development of speech and hearing of two children with Pelizaeus-Merzbacher disease presenting only waves I and II of the auditory brainstem response

MASAHIRO RIKITAKE[1] & KIMITAKA KAGA[2]

[1]*Department of Otorhinolaryngology, Jikei University School of Medicine, Minato-ku, Tokyo and* [2]*National Institute of Sensory Organs, National Tokyo Medical Center, Meguro-ku, Tokyo, Japan*

Abstract

Pelizaeus-Merzbacher disease (PMD) is a white matter dystrophy of the brain. Most children with PMD require comprehensive nursing care. Their speech and language abilities are poor or absent. Therefore, evaluating hearing ability is difficult in children with PMD. We have followed up two patients with PMD since early childhood. Patient 1 is an 11-year-old boy, and patient 2 is a 15-year-old adolescent boy in whom horizontal nystagmus was recognized after birth. Magnetic resonance imaging showed diffuse dysmyelination of the cerebral white matter. Auditory brainstem response recordings showed only waves I and II and the absence of all subsequent components. However, conditioned orientation reflex audiometry showed a threshold of 20–30 dB. Both patients can converse orally and have auditory perception and speech abilities better than those of most patients with PMD in the literature. We report on the development of their hearing and speech abilities.

Keywords: *Language, audiometry, white matter dystrophy*

Introduction

Pelizaeus-Merzbacher disease (PMD) is white matter dystrophy. It was described clinically by Pelizaeus in 1885 [1] and Merzbacher in 1910 [2], and its neuropathologic features were later described by Seitelberger [3]. In most patients with PMD, the initial signs appear during the first months of life, with pendular nystagmus followed by symptoms such as spasticity of the lower limbs, athetotic movements, and motor ataxia [4,5]. Most patients with PMD require comprehensive nursing care and cannot speak. Genetic tests and magnetic resonance imaging (MRI) are useful for diagnosis. PMD is a recessively inherited X-linked disease caused by a mutation of the proteolipid protein 1 (*PLP1*) gene on chromosome Xq22 [6]. The mutation causes hypoplastic myelination of the central nervous system, but the neurons and axons are preserved. The degree of myelination of the white matter of the brain in PMD can be evaluated with MRI, which shows a reversal of signal strength on T1-weighted and T2-weighted images. On the basis of symptom severity, PMD has been divided into six forms [7].

Evaluation of the hearing of PMD patients can be difficult. Reactions with conditioned orientation response (COR) audiometry can be unclear. Auditory brainstem response (ABR) recordings show only wave I or waves I and II. In most patients with PMD, auditory perception and comprehension of conversation are poor. The pathogenesis of PMD is poorly understood. We report, from the viewpoints of otology and neuro-otology, on two school-age children with PMD who we have followed up for many years. They have better hearing perception and speech ability than most patients with PMD and can converse orally.

Correspondence: Masahiro Rikitake MD, Department of Otorhinolaryngology, Jikei University School of Medicine, 3-25-8 Nishi-shinbashi, Minato-ku, Tokyo, 105-8461, Japan. Tel: +81 3 3433 1111. Fax: +81 3 3578 9208. E-mail: rikitake@jikei.ac.jp

(Received 22 October 2011; accepted 20 November 2011)

ISSN 0001-6489 print/ISSN 1651-2251 online © 2012 Informa Healthcare
DOI: 10.3109/00016489.2011.647362

Case reports

Patient 1

The patient is an 11-year-old boy.

First year of life: He was born after a gestation period of 38 weeks 2 days with a birth weight of 2856 g. There was no family history of genetic disorders or hearing loss. Horizontal nystagmus and cervical hypotonia were recognized soon after birth. At 2 months of age, ABR recording revealed only waves I and II in both ears (Figure 1). The DPOAEs were within the normal range in both ears. Recording of DPs showed that all DP levels (range 5–15 dB) were higher than the noise floor levels at all frequencies. The mean hearing threshold, as determined with COR audiometry at 4 months of age, was 60 dB (Figure 2). Diffuse high-intensity signals were observed on T2-weighted MRI of the white matter of the brain (Figures 3 and 4). With the consent of the patient's parents, genetic testing was performed. On the basis of the finding of duplication of the PLP gene and of the symptoms, classic PMD was diagnosed.

The development of the patient's hearing and speech is outlined below.

1 year old: He produced sounds but no meaningful words.

2 years old: He could communicate by gestures, laughing, and crying. He did not produce meaningful words.

3–4 years old: His mother observed him responding to spoken words, so she believed that he heard and understood them. He became able to pronounce single syllables that stood for words. For example, he said 'da-' instead of '*dakko*,' (meaning 'hug' in Japanese) and 'go-' instead of '*ringo*' (meaning

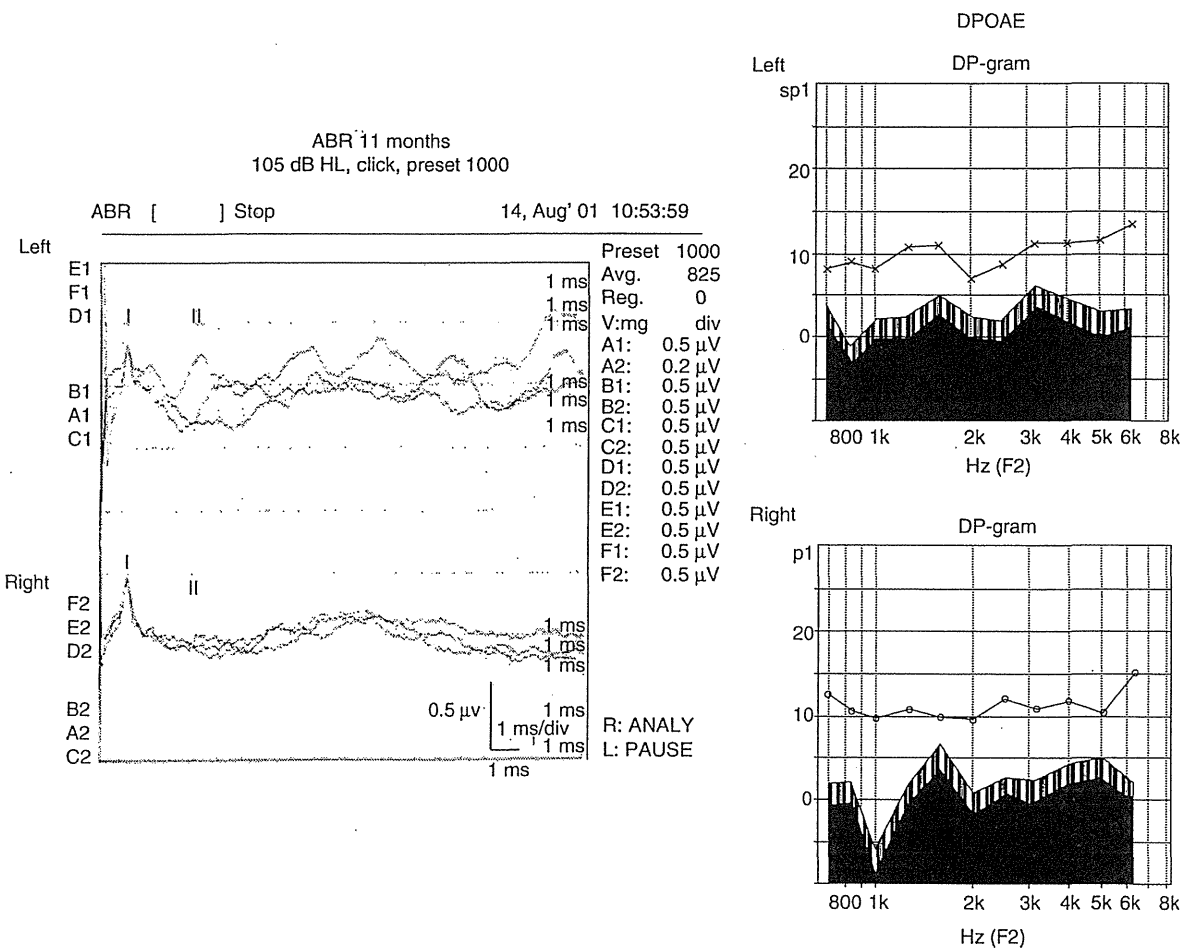

Figure 1. Patient 1. Auditory brainstem responses (ABRs) show poor waveforms at wave I and later. Distortion product otoacoustic emissions (DPOAEs) show a normal reaction.

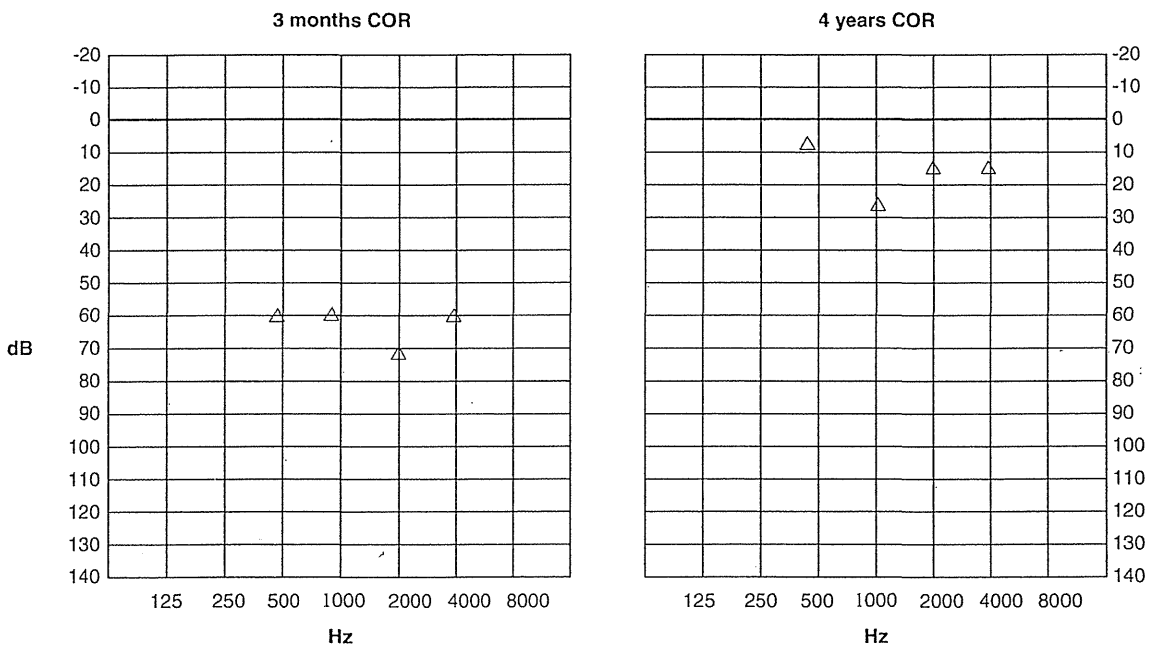

Figure 2. Patient 1. Behavior observation audiometry shows 60–70 dB at 3 months. Conditioned orientation response (COR) audiometry shows 15–25 dB at 4 years.

'apple'). He could understand the speech of others and could clearly reply by gestures of his hands or other body parts or by voice. He tried to speak, but the articulation was not clear. The mean hearing threshold on COR audiometry improved to 20–30 dB. A detailed evaluation of words and sentences was not yet possible.

6 years old: His pronunciation became clear, and he was able to talk well. He could also sing. However, the rate of speech was extremely slow, and the intonation was vague. He could write letters when his arm was supported.

8 years old: He could communicate through conversation. He could read and understand Japanese

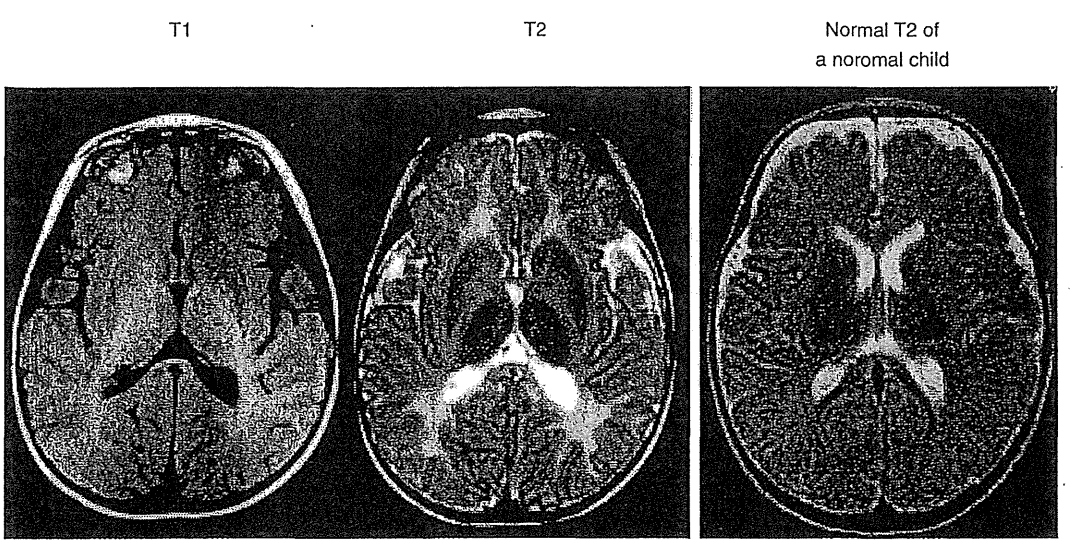

Figure 3. Patient 1. MRI of the brain at 5 months. Axial T1-weighted image (left) shows a nearly identical high-signal intensity in the internal capsule. A T2-weighted image (center) shows a diffuse high-intensity signal in white matter of brain. The MRI on the right is a normal brain at 5 months of age.

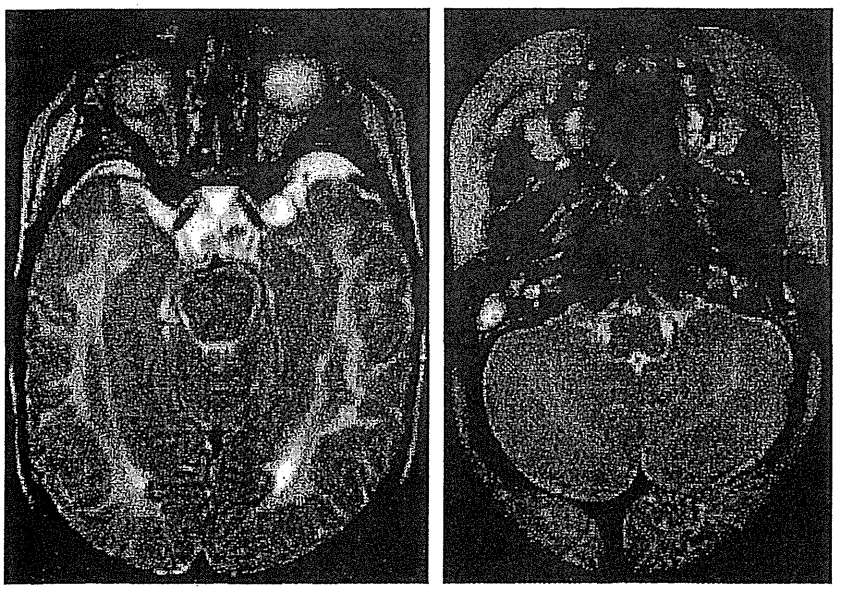

Figure 4. Patient 1. MRI of the brain at 5 months (level of brainstem).

hiragana letters. He could count from 1 to 20. The Tanaka-Kanichi (TK) development test (a Japanese test of infant development) showed that his mental age was 54 months, and his IQ was 57 months.

The patient is now 11 years old. He is in the sixth grade of a public elementary school. The Tsumori Inage development screening test (a Japanese test of infant development) showed a development level equivalent to 66 months by speech, 54 months by social function, and 42 months by exercise. With a mild degree of developmental disability, the patient undergoes speech, language, and physical therapy at a local rehabilitation center.

Patient 2

The patient is a 13-year-old adolescent boy.

First year of life: He had no family history of hearing loss or genetic disorders. Three months after birth horizontal nystagmus and cervical hypotonia were recognized. At the age of 8 months, ABR showed only waves I and II in both ears (Figure 5). The DPOAEs were within the normal range on both sides. Diffuse high-intensity signals were observed on T2-weighted MRI of the white matter of the brain (Figure 6). On the basis of symptoms and a *PLP* gene mutation revealed by genetic testing, classic PMD was diagnosed.

The development of the patient's hearing and speech is outlined below.

2 years old: The mean hearing threshold on COR audiometry was 35 dB (Figure 5). The new TK development test showed developmental levels equivalent to 11 months by exercise and posture, 21 months by recognition and adaptation, 19 months by language and social function, and 30 months by all domains. The developmental quotient was 63. He could repeat words spoken by his mother. He could speak slowly, but pronunciation was clear. He underwent speech, language, and physical therapy at a local rehabilitation center.

4 years old: His pronunciation became clearer and his conversation was age equivalent.

5 years old: The TK development test showed that the patient's calendar age was equivalent to 5 years 8 months, mental age was 5 years 1 month, and IQ was 90. A delay for the development of word use and intellect was not recognized.

7 years old: He entered a class for handicapped children at a public elementary school and participated in regular classes with other children.

11 years old: He could write a composition and send e-mails with a mobile phone. His pronunciation was clear.

12 years old: He completed elementary school and now attends a public junior high school. He did not have any problem communicating in conversation.

Audiological examinations

COR audiometry. To evaluate hearing, patients underwent COR audiometry inside an electrically shielded sound-attenuating room.

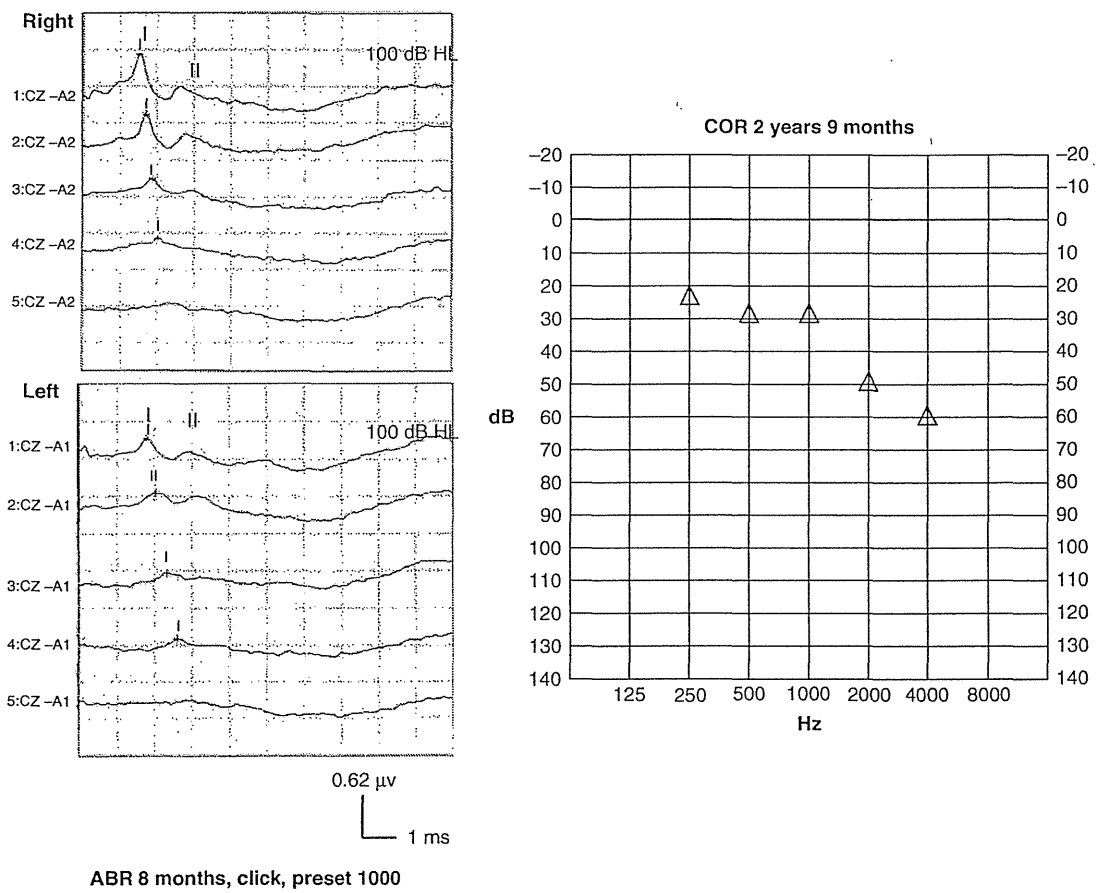

Figure 5. Patient 2. Auditory brainstem responses (ABRs) show poor waveforms for wave II and later. Conditioned orientation response (COR) audiometry shows 25–60 dB at 2 years 9 months.

Distortion product otoacoustic emissions. Patients were tested inside an electrically shielded sound-attenuating room. Distortion product (DP) otoacoustic emissions (OAEs) were recorded and analyzed with an ILO92 OAE dynamic analyzer system (Otodynamics Ltd, Hatfield, UK).

ABRs. Examinations were performed with the patients in the supine position under sedation with trichloryl chloride. Silver disk electrodes placed on each patient's forehead were referenced to the mastoid tip on the tested side and were connected to the ground on the opposite mastoid tip. Each click

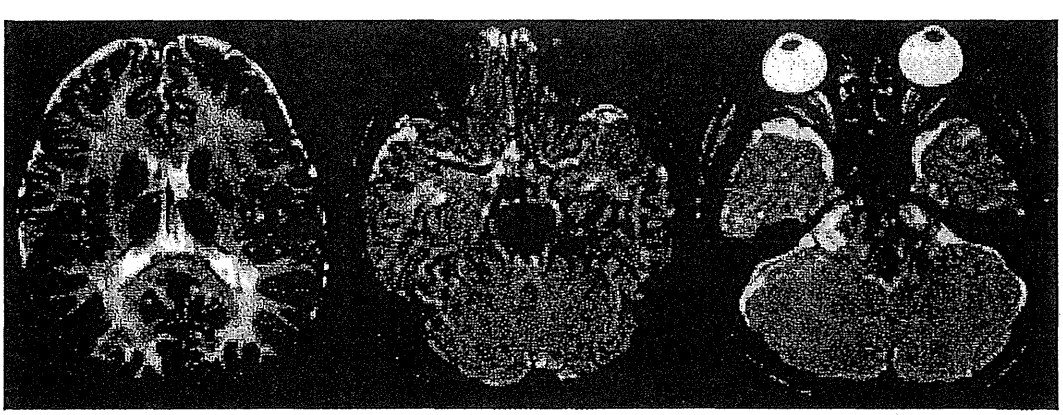

Figure 6. Patient 2. T2-weighted MRI showing a high-intensity signal in the subcortical area.

stimulus was presented for one cycle of a 3000 Hz sine wave. Monaural headphones delivered 1000 clicks at a rate of 10 clicks per second. The stimulus intensities were 105 dB above the normal adult hearing level (nHL) for patient 1 and 100 dB nHL for patient 2. The data were averaged, displayed, and recorded with an online computer.

Discussion

PMD is an extremely rare disease, with frequency of about 1 in 300 000 persons. A standard treatment for PMD has not been established. PMD has been classified on the basis of symptoms into six types: type 1, classic PMD; type 2, connatal type; type 3, transitional type between classic and connatal types; type 4, adult Löwenberg-Hill type; type 5, variant type with patchy demyelination; and type 6, demyelination variant type in Cockayne's syndrome. However, the distinctions between types are not clear, and patients may shift between types. Ellis and Malcolm have reported that symptoms differ with the degree of duplication of *PLP* gene mutations [8]. Variable expressivity of the *PLP* gene mutation may have an effect on the degree of dysmyelination.

The brains of healthy neonates contain a large amount of water, which is a characteristic of undeveloped white matter. Therefore, in the cerebral white matter T1-weighted MRI shows low-intensity signals, and T2-weighted MRI shows high-intensity signals. With maturation, myelination develops in the cerebral white matter, the low-intensity signals seen on T1-weighted MRI are replaced by high-intensity signals, and the high-intensity signals on T2-weighted MRI are replaced by low-intensity signals. In the brains of patients with PMD, the delayed myelination of white matter is recognized with MRI. As described by Holland et al. [9], in a healthy child myelination of the cortical white matter is distinguished from the nearby cortical gray matter from 4 to 6 months after birth. By 9 months to 1 year after birth, the myelination of the cortex is the same as in adults. In patients with PMD, including both our patients, myelination of the posterior limb of the internal capsule is not recognized (in a healthy child, myelination of the posterior limb of the internal capsule is recognized with MRI 1–2 months after birth). Myelination is considered to be present in the white matter if the signal in unmyelinated white matter is hypointense on T2-weighted spin-echo MRI. Myelination is considered to be present in the cortical gray matter structures if the signal is hypointense on T2-weighted spin-echo MRI [10].

On the basis of symptoms and the results of MRI, ABR recordings, and genetic analysis, both our patients are thought to have classic PMD. Because of paralysis and ataxia, most patients with PMD require comprehensive nursing care. They usually have hearing loss and cannot speak because of disorders of articulation. However, both our patients hear and speak well.

Hearing in both patients was examined with COR audiometry and DPOAE and ABR recording. On COR audiometry, response thresholds of 40–60 dB were recognized at an early age in both patients. As the patients matured, the response threshold improved to 20–30 dB. The reactions to DPOAEs were normal. Recording of ABRs showed only waves I and II. However, DPOAE and ABR recordings revealed that cochlear functions in both patients were normal.

The hearing loss in patients with PMD is thought to be caused by an isolated disorder of myelination. A normal axon is covered by a myelin sheath, and stimulation occurs through saltatory conduction. The conduction speed in the healthy nervous system is 50–430 km/h, but without myelination, the conduction speed is around 2.0 km/h. In patients with PMD, nerve stimulation is insufficient for saltatory conduction, and the stimuli are conducted at different speeds in each nerve cell. Because the stimulation does not synchronize, the wave pattern after waves I and II of ABR does not appear. Therefore, after waves I and II the wave becomes flat. In patients with PMD who hear well (such as our patients), central hearing tests (e. g. magnetoencephalography and functional MRI) will show normal reactions. These patients can communicate through oral conversation. Their cognitive hearing ability is not poor, even though they show only ABR waves I and II.

We have reported on two unusual patients with PMD who can hear and speak well despite ABR recording showing only waves I and II. In our patients, because the degree of dysmyelination is slight, the disorder of saltatory conduction of neurons is also slight. The stimulation does not synchronize, but sound stimuli are conducted from the inner ear to auditory areas of brain. In addition, ABR is a reaction to click stimuli, but the auditory pathway except for the click part of the sound pathway is not abnormal. Other gene mutations may also affect myelination. Differences in the degree of dysmyelination are thought to be responsible for the differences in symptoms that cause PMD to be classified as different types. The hearing loss in PMD is completely unlike the hearing loss due to acoustic neuromas and brainstem disorders. The hearing function and language abilities of patients with PMD should be carefully observed so that their quality of life can be improved.

Declaration of interest: The authors report no conflicts of interest. The authors alone are responsible for the content and writing of the paper.

References

[1] Pelizaeus F. Ueber eine eigenthümliche Form spastischer Lähmung mit Cerebralerscheinungen auf hereditärer Grundlage (Multiple Sklerose). Arch Psychiatr Nervenklankf 1885; 16:698–710.

[2] Merzbacher L. Eine eigenartige familiar-hereditare Erkrankungsform (Aplasia axialis extracorticalis congenita). Zeiaschr Ges Neurol Psychiatr 1910;3:100–38.

[3] Seitelberger F. Pelizaeus-Merzbacher disease. 1970. In: Vinken PJ, Bruyn GW, editors. Handbook of clinical neurology. Leucodystrophies and poliodystrophies. Amsterdam: North-Holland. p 150–202.

[4] Kaga K, Tamai F, Kodama M, Kodama K. Three young adult patients with Pelizaeus-Merzbacher disease who showed only waves I and II in auditory brainstem responses but had good auditory perception. Acta Otolaryngol 2005; 125:1018–23.

[5] Kaga K, Kenji Y, Eiji K, Kazuo K, Roger M. Absence of later auditory brain stem response components, congenital horizontal nystagmus, and hypotonia in male infants. Ann Otol Rhinol Laryngol 1986;95:203–6.

[6] Inoue K. PLP1-related inherited dysmyelinating disorders: Pelizaeus-Merzbacher disease and spastic paraplegia type 2. Neurogenetics 2005;6:1–16.

[7] Allen IV. Pelizaeus-Merzbacher disease. 1984. In: Adams J, Corsellis JAN, Duchen LLW, editors. Greenfield's neuropathology, 4th edition. London: Edward Arnold. p 371–3.

[8] Ellis D, Malcolm S. Proteolipid protein gene dosage effect in Pelizaeus-Merzbacher disease. Nat Genet 1994;6:333–4.

[9] Holland BA, Haas DK, Norman D, Brant Zawadzki M, Newton TH. MRI of normal brain maturation. AJNR 1986;7:201–8.

[10] Barcovich AJ. MR of the normal neonatal brain: assessment of deep structures. AJNR Am J Neuroradiol 1998;19: 397–403.

Acta Oto-Laryngologica, 2012; Early Online, 1–7

informa
healthcare

ORIGINAL ARTICLE

Genetic analysis of *PAX3* for diagnosis of Waardenburg syndrome type I

TATSUO MATSUNAGA[1], HIDEKI MUTAI[1], KAZUNORI NAMBA[1], NORIKO MORITA[2] & SAWAKO MASUDA[3]

[1]*Department of Otolaryngology, Laboratory of Auditory Disorders, National Institute of Sensory Organs, National Tokyo Medical Center, Tokyo,* [2]*Department of Otolaryngology, Teikyo University School of Medicine, Tokyo and* [3]*Department of Otorhinolaryngology, Institute for Clinical Research, National Mie Hospital, Tsu, Japan*

Abstract

Conclusion: PAX3 genetic analysis increased the diagnostic accuracy for Waardenburg syndrome type I (WS1). Analysis of the three-dimensional (3D) structure of PAX3 helped verify the pathogenicity of a missense mutation, and multiple ligation-dependent probe amplification (MLPA) analysis of *PAX3* increased the sensitivity of genetic diagnosis in patients with WS1. *Objectives:* Clinical diagnosis of WS1 is often difficult in individual patients with isolated, mild, or non-specific symptoms. The objective of the present study was to facilitate the accurate diagnosis of WS1 through genetic analysis of *PAX3* and to expand the spectrum of known *PAX3* mutations. *Methods:* In two Japanese families with WS1, we conducted a clinical evaluation of symptoms and genetic analysis, which involved direct sequencing, MLPA analysis, quantitative PCR of *PAX3*, and analysis of the predicted 3D structure of PAX3. The normal-hearing control group comprised 92 subjects who had normal hearing according to pure tone audiometry. *Results:* In one family, direct sequencing of *PAX3* identified a heterozygous mutation, p. I59F. Analysis of PAX3 3D structures indicated that this mutation distorted the DNA-binding site of PAX3. In the other family, MLPA analysis and subsequent quantitative PCR detected a large, heterozygous deletion spanning 1759–2554 kb that eliminated 12–18 genes including a whole *PAX3* gene.

Keywords: *Mutation, MLPA, clinical diagnosis, hearing loss, dystopia canthorum, pigmentary disorder*

Introduction

Waardenburg syndrome (WS) is a hereditary auditory pigmentary disorder that is responsible for 1–3% of congenital deafness cases [1]. WS is classified into four types based on symptoms other than the auditory and pigmentary disorder. Type I WS (WS1) includes dystopia canthorum, and this feature distinguishes WS1 from type II WS. Type III WS is similar to WS1 but is associated with musculoskeletal anomalies of the upper limbs. Type IV WS is similar to type I but is associated with Hirschsprung disease. Diagnostic criteria for WS1 have been proposed [2]. The clinical features of WS1 demonstrate incomplete penetrance and highly varied expression [3,4], which makes diagnosis in individual patients challenging. For example, WS1 patients may present only one isolated symptom. Diagnosis of high nasal root and medial eyebrow flare can be difficult when they are mild. Hearing loss and early graying are relatively common in the general population and are not specific to WS1. Thus, the accuracy of WS1 diagnosis needs to be improved by the use of additional diagnostic procedures.

It is reported that more than 90% of patients with WS1 harbor point mutations in *PAX3* [5], and an additional 6% of WS1 patients harbor partial or complete *PAX3* deletions [6]. This high frequency of *PAX3* mutation in WS1 suggests that clinical diagnosis of WS1 could be facilitated by *PAX3* genetic analysis. To date, more than 80 *PAX3*

Correspondence: Tatsuo Matsunaga, Department of Otolaryngology, Laboratory of Auditory Disorders, National Institute of Sensory Organs, National Tokyo Medical Center, 2-5-1 Higashigaoka, Meguro, Tokyo, 152-8902, Japan. Tel: +81 3 3411 0111. Fax: +81 3 3412 9811. E-mail: matsunagatatsuo@kankakuki.go.jp

This study was presented at the annual meeting of the Collegium Oto-Rhino-Laryngologicum Amicitiae Sacrum, Rome, August 28, 2012.

(Received 19 September 2012; accepted 20 October 2012)

ISSN 0001-6489 print/ISSN 1651-2251 online
DOI: 10.3109/00016489.2012.744470

mutations are reported to be associated with WS1 [5]. A de novo paracentric inversion on chromosome 2 in a Japanese child with WS1 provided a clue for identification of *PAX3* in the distal part of chromosome 2 [7]. However, only a few *PAX3* mutations including the chromosomal inversion have been reported in Japanese patients with WS1 since then [8,9].

In the present study, we conducted *PAX3* genetic analysis to facilitate diagnosis of WS1 in two Japanese families. In one family, to verify the pathogenicity of an identified missense mutation, we analyzed the effect of the mutation on the three-dimensional (3D) structure of PAX3. In the other family, no mutations were identified by direct sequencing, so multiple ligation-dependent probe amplification (MLPA) analysis was used to search for large deletions in *PAX3* and thereby increase the sensitivity of genetic diagnosis.

Material and methods

Patients and control subjects

Two Japanese families with WS1 were included in the study. The diagnosis of WS1 was based on criteria proposed by the Waardenburg Consortium [2]. The normal-hearing controls comprised 92 subjects who had normal hearing according to pure tone audiometry. This study was approved by the institutional ethics review board at the National Tokyo Medical Center. Written informed consent was obtained from all subjects included in the study or from their parents.

Clinical evaluation

A comprehensive clinical history was taken from subjects who were examined at our hospitals or from their parents. During physical examination, special attention was given to the color of the skin, hair, and iris, and to other anomalies such as dystopia canthorum, medial eyebrow flare, limb abnormalities, and Hirschsprung disease. After otoscopic examination, behavioral audiometric testing was performed. The test protocol was selected according to the developmental age of the subject (conditioned orientation response audiometry, play audiometry, or conventional audiometric testing, from 125 to 8000 Hz), and testing was performed using a diagnostic audiometer in a soundproof room. Auditory brainstem response (ABR) and otoacoustic emission were also evaluated in some subjects.

Direct sequencing

Genomic DNA from the subjects was extracted from peripheral blood leukocytes using the Gentra Puregene® Blood kit (QIAGEN, Hamburg, Germany). Mutation screening of *PAX3* was performed by bidirectional sequencing of each exon (exons 1–11) together with the flanking intronic regions using an ABI 3730 Genetic Analyzer (Applied Biosystems, Foster City, CA, USA). Primer sequences for *PAX3* are listed in Table I. Mutation nomenclature is based on the genomic DNA sequence of [GenBank accession no. NG_011632.1], with the A of the translation initiation codon considered as +1. Nucleotide conservation between mammalian species was evaluated using ClustalW (http://www.ebi.ac.uk/Tools/msa/clustalw2/). PolyPhen-2 software (http://genetics.bwh.harvard.edu/pph2/) was used to predict the functional consequence(s) of each amino acid substitution.

MLPA

MLPA analysis was performed using an MLPA kit targeting *PAX3*, *MITF*, and *SOX10* (SALSA MLPA Kit P186-B1, MRC-Holland, Amsterdam, The Netherlands) according to the manufacturer's protocol. Exon-specific MLPA probes for exons 1–9 of *PAX3* and control probes were hybridized to genomic DNA from the subjects and normal controls and ligated with fluorescently labeled primers. A PCR reaction was then performed to amplify the hybridized probes. The amplified probes were fractionated on an ABI3130xl Genetic Analyzer (Applied Biosystems) and the peak patterns were evaluated using GeneMapper (Applied Biosystems).

Real-time PCR

To determine the length of each deleted genomic region, 100 ng of genomic DNA from the subjects and a normal control were subjected to quantitative PCR (Prism 7000, Applied Biosystems) using Power SYBR® Green Master Mix (Life Technologies, Carlsbad, CA, USA) and 12 sets of primers designed to amplify sequence-tagged sites on chromosome 2 (GenBank accession nos: RH46518, RH30035, RH66441, GDB603632, 1988, RH24952, RH47422, RH65573, RH26526, RH35885, RH16314, and RH92249).

Homology modeling of the PAX3 paired domain

The DNA-binding site of the paired domain of PAX3 was modeled using SWISS-MODEL [10] with the crystal structure of the PAX5 paired domain-DNA complex (PDB ID:1PDN_chain C) as the template because PAX3 and PAX5 are functionally and structurally similar [11]. The amino acid

Table I. Primer sequences for *PAX3*.

Exon 1	Forward	5′-TGTAAAACGACGGCCAGTAGAGCAGCGCGCTCCATTTG-3′
	Reverse	5′-CAGGAAACAGCTATGACCGCTCGCCGTGGCTCTCTGA-3′
Exon 2	Forward	5′-TGTAAAACGACGGCCAGTAAGAAGTGTCCAGGGCGCGT-3′
	Reverse	5′-CAGGAAACAGCTATGACCGGTCTGGGTCTGGGAGTCCG-3′
Exon 3	Forward	5′-TGTAAAACGACGGCCAGTTAAACGCTCTGCCTCCGCCT-3′
	Reverse	5′-CAGGAAACAGCTATGACCGGGATGTGTTCTGGTCTGCCC-3′
Exon 4	Forward	5′-TGTAAAACGACGGCCAGTAATGGCAACAGAGTGAGAGCTTCC-3′
	Reverse	5′-CAGGAAACAGCTATGACCAGGAGACACCCGCGAGCAGT-3′
Exon 5	Forward	5′-TGTAAAACGACGGCCAGTGGTGCCAGCACTCTAAGAACCCA-3′
	Reverse	5′-CAGGAAACAGCTATGACCGGTGATCTGACGGCAGCCAA-3′
Exon 6	Forward	5′-TGTAAAACGACGGCCAGTTGCATCCCTAGTAAAGGGCCA-3′
	Reverse	5′-CAGGAAACAGCTATGACCGGTGTCCATGGAAGACATTGGG-3′
Exon 7	Forward	5′-AACTATTATTTCATCAGTGAAATC-3′
	Reverse	5′-ATTCACTTGTATAAAATATCCACC-3′
Exon 8	Forward	5′-TGTAAAACGACGGCCAGTTGAAGCCAGTAGGAAGGGTGGA-3′
	Reverse	5′-CAGGAAACAGCTATGACCTGCAGGTTAAGAAACGCAGTTTGA-3′
Exon 9a	Forward	5′-TGTAAAACGACGGCCAGTTTGATACCGGCATGTGTGGC-3′
	Reverse	5′-CAGGAAACAGCTATGACCTGCAGTCAGATGTTATCGTCGGG-3′
Exon 9b	Forward	5′-TGTAAAACGACGGCCAGTCACAACTTTGTGTCCCTGGGATT-3′
	Reverse	5′-CAGGAAACAGCTATGACCGGGACTCCTGACCAACCACG-3′
Exon 10–11	Forward	5′-TGTAAAACGACGGCCAGTGCAAATGGAATGTTCTAGCTCCTCG-3′
	Reverse	5′-CAGGAAACAGCTATGACCGGTCAGCTCCAGGATCATATGGG-3′

sequences of the PAX3 and PAX5 paired domains were 79% homologous. The predicted PAX3 structure and the p.I59F mutation structure were superimposed on the backbone atoms of the PAX5 paired domain-DNA complex and displayed using the extensible visualization system, UCSF Chimera [12].

Results

In family 1, the proband, a 9-month-old male, was the first child of unrelated Japanese parents. Abnormal responses were found upon newborn hearing screening in the left ear, and left hearing loss was diagnosed by ABR. On physical examination, dystopia canthorum was noted, with a W-index of 2.77. The patient's mother also had dystopia canthorum, with a W-index of 2.68. She also had a history of early graying that started at age 16 years. She had not been diagnosed with WS1. According to the parents, 10 members of this family, including the proband and the mother, showed clinical features consistent with WS1 (Figure 1). ABR performed in the proband

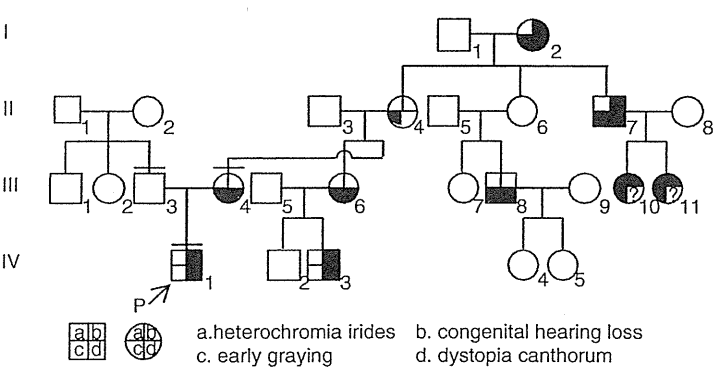

Figure 1. Pedigree of family 1. The proband is indicated by an arrow. The individuals we examined personally are indicated by a bar over the symbol. Phenotypes observed in this family are indicated symbolically as detailed below the pedigree.

revealed normal hearing in the right ear and no responses to 105 dB click stimuli in the left ear. Computed tomography (CT) of the temporal bone showed normal structures in the inner, middle, and outer ears.

Genetic analysis of *PAX3* was conducted in this family, and direct sequencing of *PAX3* revealed a heterozygous mutation, c.175A>T, in the proband and his mother. This mutation resulted in a missense mutation, p.I59F (Figure 2A). The proband's father did not harbor this mutation. p.I59F is located within exon 2 and is part of the paired domain of *PAX3*, which is a critical region for interaction between transcription factors and target DNA (Figure 2B). A multiple alignment of *PAX3* orthologs at this region demonstrated that I59 was evolutionarily conserved among various species (Figure 2C). The p.I59F mutation was not identified in any of the 184 alleles from the normal control subjects. This mutation was predicted to be 'probably damaging' according to PolyPhen-2 software.

The predicted 3D structures of the paired domain of the PAX3-DNA complex indicated that the PAX3 paired domain binds to the corresponding DNA (white double helixes) via hydrogen bonds (pink lines) at the N-terminal of α-helix1 (H1), α-helix2 (H2), and α-helix3 (H3) (indicated in blue; Figure 3A). I59 is located in the middle of H1, H2, and H3 and is surrounded by hydrophobic residues (green) protruding from H1, H2, and H3. Because the van der Waals radius of phenylalanine (Figure 3C; white arrows) is larger than that of isoleucine (Figure 3B, white arrowheads), F59 repels the surrounding hydrophobic residues by van der Waals forces and increases the distance between F59 and the surrounding hydrophobic residues, resulting in structural distortion of the DNA-binding site of PAX3. Since this site is precisely shaped for maximal binding to the corresponding DNA, this mutation is likely to reduce the binding ability of the paired domain of PAX3 and cause WSI. A mutational search found the same mutation in another Japanese family [8].

In family 2, the proband, a female aged 4 years and 4 months, was the first child of unrelated Japanese parents. Abnormal responses were found upon newborn hearing screening in the right ear, and right hearing loss was diagnosed by ABR. On physical examination, dystopia canthorum, medial eyebrow flare, and a white forelock were noted. She was admitted to hospital suffering from ketotic hypoglycemia of unknown cause when aged 4 years. Her mother presented with heterochromia iridis, dystopia canthorum, and medial eyebrow flare, and her grandmother presented with early graying that started at around 20 years of age, dystopia canthorum, and

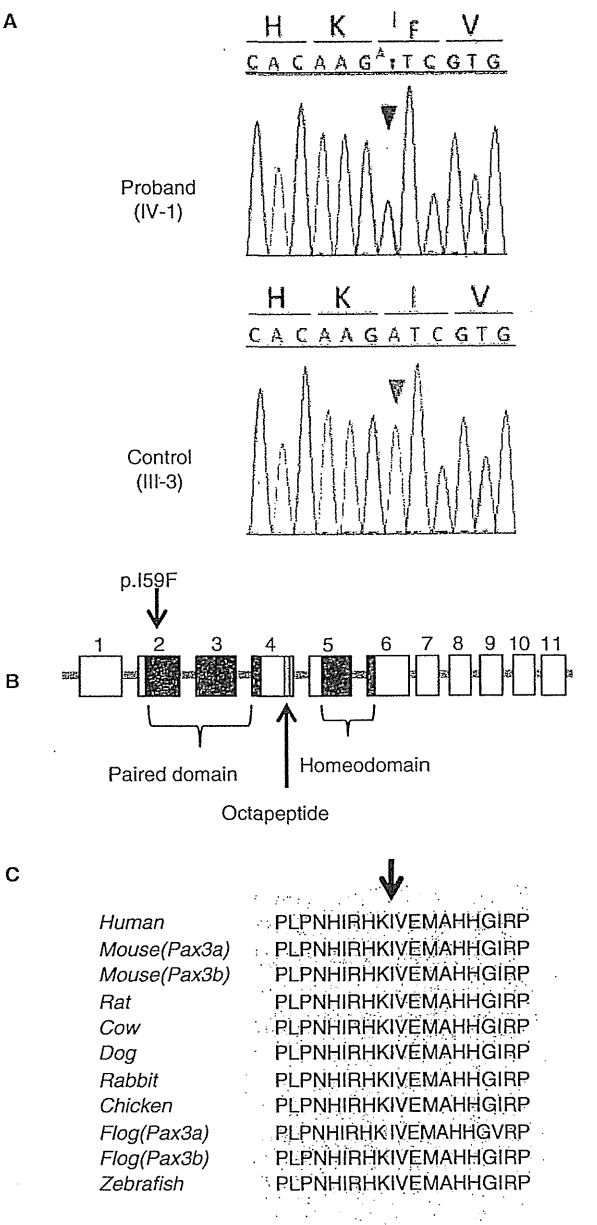

Figure 2. The p.I59F mutation of *PAX3* detected in family 1. (A) Sequence chromatogram for the proband and unaffected control. A heterozygous A to T transversion (red arrowhead) that changes codon 59 from ATC, encoding isoleucine (I), to TTC, encoding phenylalanine (F), was detected in the proband but not in the control (green arrowhead). (B) Localization of the p.I59F mutation and functional domains of PAX3. (C) A multiple alignment of PAX3 orthologs. Regions of amino acid sequence identity are shaded gray. The position of I59 is indicated by an arrow and shaded yellow.

medial eyebrow flare. According to the grandmother, the father of the grandmother also had dystopia canthorum and medial eyebrow flare. The pedigree of family 2 is shown in Figure 4. The grandmother

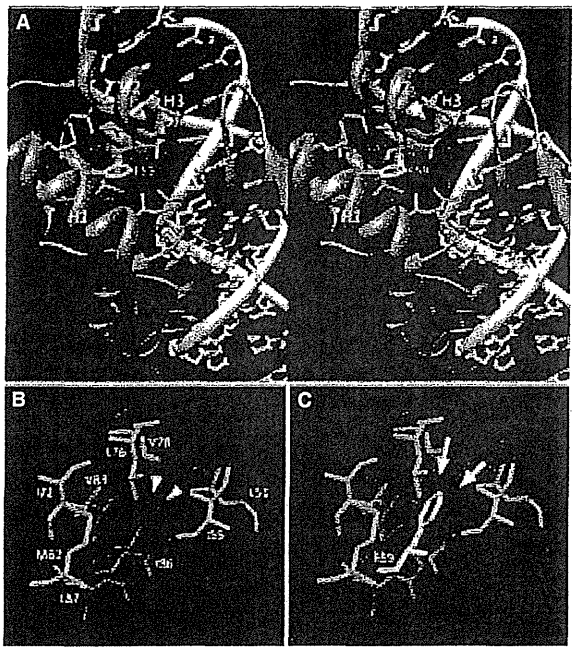

Figure 3. The predicted structure of the PAX3 paired domain-DNA complex. (A) The stereo view indicates that the mutated residue was surrounded by hydrophobic residues (green) protruding from H1, H2, and H3 of the paired domain (blue), which binds to DNA (white, sugar; blue, nitrogen; red, oxygen). The pink lines indicate hydrogen bonds. Magenta and yellow residues indicate I59 and F59, respectively. (B, C) The colored spheres indicate the van der Waals surface boundaries, the radius of the hydrophobic residues is shown in green, I59 is shown in magenta and is also indicated by arrowheads, and F59 is shown in yellow and is also indicated by arrows.

and her father had never been diagnosed with WS1. Pure tone audiometry of the proband showed severe hearing loss in the right ear and normal hearing in the left ear. The results of ABR and distortion product otoacoustic emissions in the proband were compatible with those obtained for pure tone audiometry.

Because direct sequencing of *PAX3* in the proband and her grandmother revealed no mutations, we conducted MLPA analysis to search for a large deletion of *PAX3*, and found that the copy number of all tested exons (exons 1–9) of *PAX3* was half that of the number of other chromosomal regions in both subjects (Figure 5A). In control subjects, all tested exons of *PAX3* showed the same copy number as the other chromosomal regions (Figure 5B). To determine the size of the deleted region, quantitative PCR was performed at 12 sequence-tagged sites on chromosome 2q36, which includes *PAX3*. In the proband, copy numbers at nine sites in the middle of the tested region (white arrows) were half that of those examined in normal controls, but the copy numbers at three of the sites near the 5' and 3' ends of the tested region (black arrows) were identical to those examined in normal controls (Figure 6). This result demonstrated that the chromosomal region spanning 1759–2554 kb at 2q36, which includes the whole *PAX3* gene, was deleted in one of the alleles of the proband. The same results were detected in the grandmother. A search for the deleted region revealed that this region contained between 12 and 18 genes, including *PAX3*.

Discussion

The heterozygous missense mutation, p.I59F, was identified in family 1. The pathogenicity of a novel or rare missense mutation in the causative gene is not necessarily verified even when the mutation is absent from a large number of normal controls, when the residue is evolutionary conserved among different species, or if the mutation is associated with the phenotype within a family, because an identified

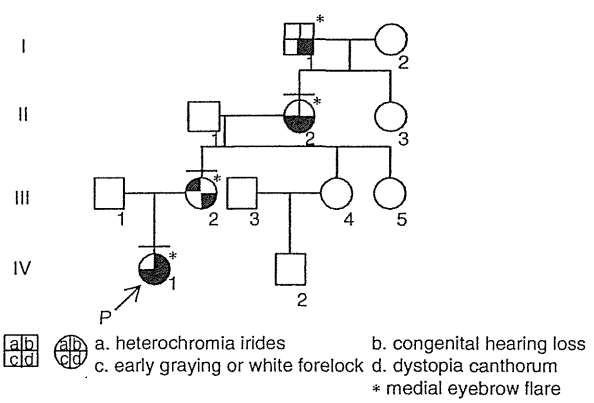

Figure 4. Pedigree of family 2. The proband is indicated by an arrow. The individuals we examined personally are indicated by a bar over the symbol. Phenotypes observed in this family are indicated symbolically, as detailed below the pedigree.

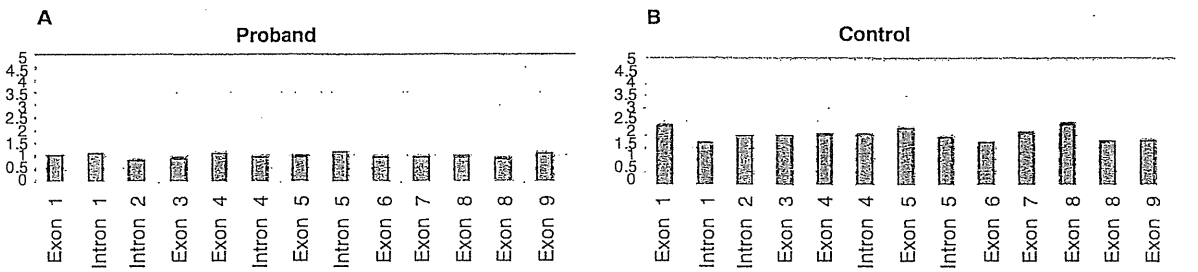

Figure 5. Results of MLPA analysis of *PAX3* in family 2. (A, B) Relative ratios of DNA quantity in each exon compared with that in the control region are shown for the proband (A) and control (B).

missense mutation may be a rare normal variant. Thus, the pathogenicity of such mutations needs to be verified by detection of the same mutation in multiple families with the same phenotype or by functional analysis. The functional consequences of a few *PAX3* mutations have been tested and reduced DNA-binding properties have been reported [13–15]. The p.I59F mutation was reported in a Japanese family [8], but functional analysis has not been conducted. We analyzed the predicted 3D structures of the paired domain of the PAX3-DNA complex and showed that this mutation was likely to distort the structure of the DNA-binding site of PAX3 and lead to functional impairment. This result substantially supports the hypothesis that the p.I59F mutation is pathogenic, although it is based on a theoretical prediction rather than functional experiments.

In family 2, the distinct phenotypes of the proband, the proband's mother, and the proband's grandmother were congenital unilateral hearing loss, heterochromia iridis, and early graying, respectively. Because of these differences, they were not aware of the hereditary nature of the symptoms. Identification of the *PAX3* mutation in the proband and the proband's grandmother led to an accurate diagnosis of WS1 and facilitated understanding of the symptoms. In this family, direct sequencing of *PAX3* did not detect any mutations, but MLPA analysis detected a large heterozygous deletion. Furthermore, quantitative PCR analysis revealed that the deleted region spanned 1759–2554 kb and included 12–18 genes. Large deletions of *PAX3* in patients with WS1 have been reported in several families [6,16–18]. To our knowledge, however, this is the largest deletion identified in patients with WS1 and has, therefore, expanded the spectrum of *PAX3* mutations. There is no reported correlation between the nature of the mutation (deleted vs truncated or missense) or

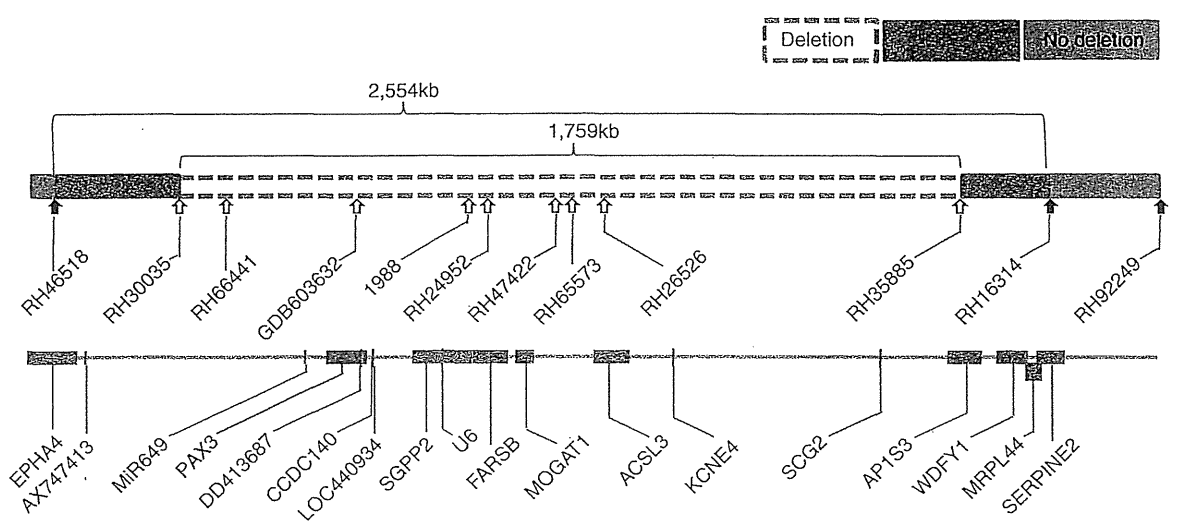

Figure 6. Genetic map showing the estimated location of the *PAX3* deletion together with the regions surrounding *PAX3*. Sites examined by quantitative PCR are indicated by arrows. Blank and white arrows indicate that the quantities of DNA at these sites are half or identical to the quantities of DNA at the corresponding sites in the control, respectively. The 5' and 3' ends of the deletion are located within the blue regions flanking the white region, designated as 'deletion,' and flanked by the green regions, designated as 'no deletion.' All genes mapped within this region, including *PAX3*, are shown in the lower map.

its location in *PAX3*, and the severity of the WS1 phenotype [19,20]. Similarly, no evidence of such a correlation was found in the data presented in this study.

In the present study, *PAX3* genetic diagnosis contributed to the accurate diagnosis of WS1. Such diagnosis could help provide genetic counseling to patients with isolated or few phenotypic symptoms, those with mild phenotypes or few first-degree relatives, or those who have yet to develop any symptoms. In addition, analysis of the predicted 3D structure of PAX3 facilitated the verification of pathogenicity of a missense mutation, and MLPA analysis increased the sensitivity of genetic diagnosis of WS1.

Acknowledgments

We thank the families that participated in this study. This study was supported by a Grant-in-Aid for Clinical Research from the National Hospital Organization, and by a Health and Labour Sciences Research Grants for Research on Rare and Intractable Diseases from the Ministry of Health, Labour and Welfare of Japan.

Declaration of interest: The authors report no conflicts of interest. The authors alone are responsible for the content and writing of the paper.

References

[1] Read AP, Newton VE. Waardenburg syndrome. J Med Genet 1997;34:656–65.

[2] Farrer LA, Grundfast KM, Amos J, Arnos KS, Asher JH Jr, Beighton P, et al. Waardenburg syndrome (WS) type I is caused by defects at multiple loci, one of which is near ALPP on chromosome 2: first report of the WS consortium. Am J Hum Genet 1992;50:902–13.

[3] Liu XZ, Newton VE, Read AP. Waardenburg syndrome type II: phenotypic findings and diagnostic criteria. Am J Med Genet 1995;55:95–100.

[4] Pardono E, van Bever Y, van den Ende J, Havrenne PC, Iughetti P, Maestrelli SR, et al. Waardenburg syndrome: clinical differentiation between types I and II. Am J Med Genet A 2003;117A:223–35.

[5] Pingault V, Ente D, Dastot-Le Moal F, Goossens M, Marlin S, Bondurand N. Review and update of mutations causing Waardenburg syndrome. Hum Mutat 2010;31: 391–406.

[6] Milunsky JM, Maher TA, Ito M, Milunsky A. The value of MLPA in Waardenburg syndrome. Genet Test 2007;11:179–82.

[7] Ishikiriyama S, Tonoki H, Shibuya Y, Chin S, Harada N, Abe K, et al. Waardenburg syndrome type I in a child with de novo inversion (2)(q35q37.3). Am J Med Genet 1989;33: 505–7.

[8] Soejima H, Fujimoto M, Tsukamoto K, Matsumoto N, Yoshiura KI, Fukushima Y, et al. Three novel PAX3 mutations observed in patients with Waardenburg syndrome type 1. Hum Mutat 1997;9:177–80.

[9] Kashima T, Akiyama H, Kishi S. Asymmetric severity of diabetic retinopathy in Waardenburg syndrome. Clin Ophthalmol 2011;5:1717–20.

[10] Kiefer F, Arnold K, Kunzli M, Bordoli L, Schwede T. The SWISS-MODEL Repository and associated resources. Nucleic Acids Res 2009;37:D387–92.

[11] Xu W, Rould MA, Jun S, Desplan C, Pabo CO. Crystal structure of a paired domain-DNA complex at 2. 5 A resolution reveals structural basis for Pax developmental mutations. Cell 1995;80:639–50.

[12] Pettersen EF, Goddard TD, Huang CC, Couch GS, Greenblatt DM, Meng EC, et al. UCSF Chimera – a visualization system for exploratory research and analysis. J Comput Chem 2004;25:1605–12.

[13] Chalepakis G, Goulding M, Read A, Strachan T, Gruss P. Molecular basis of splotch and Waardenburg Pax-3-mutations. Proc Natl Acad Sci USA 1994;91:3685–9.

[14] Corry GN, Underhill DA. Pax3 target gene recognition occurs through distinct modes that are differentially affected by disease-associated mutations. Pigment Cell Res 2005;18: 427–38.

[15] Fortin AS, Underhill DA, Gros P. Reciprocal effect of Waardenburg syndrome mutations on DNA binding by the Pax-3 paired domain and homeodomain. Hum Mol Genet 1997;6:1781–90.

[16] Baldwin CT, Lipsky NR, Hoth CF, Cohen T, Mamuya W, Milunsky A. Mutations in PAX3 associated with Waardenburg syndrome type I. Hum Mutat 1994;3:205–11.

[17] Tassabehji M, Newton VE, Leverton K, Turnbull K, Seemanova E, Kunze J, et al. PAX3 gene structure and mutations: close analogies between Waardenburg syndrome and the Splotch mouse. Hum Mol Genet 1994;3: 1069–74.

[18] Wang J, Li S, Xiao X, Wang P, Guo X, Zhang Q. PAX3 mutations and clinical characteristics in Chinese patients with Waardenburg syndrome type 1. Mol Vis 2010;16:1146–53.

[19] Baldwin CT, Hoth CF, Macina RA, Milunsky A. Mutations in PAX3 that cause Waardenburg syndrome type I: ten new mutations and review of the literature. Am J Med Genet 1995;58:115–22.

[20] Tassabehji M, Newton VE, Liu XZ, Brady A, Donnai D, Krajewska-Walasek M, et al. The mutational spectrum in Waardenburg syndrome. Hum Mol Genet 1995;4: 2131–7.

CLINICAL GENETICS An International Journal of Genetics, Molecular and Personalized Medicine

Clin Genet 2012: 82: 425–432
Printed in Singapore. All rights reserved

CLINICAL GENETICS
doi: 10.1111/j.1399-0004.2012.01897.x

Original Article

A prevalent founder mutation and genotype–phenotype correlations of *OTOF* in Japanese patients with auditory neuropathy

Matsunaga T, Mutai H, Kunishima S, Namba K, Morimoto N, Shinjo Y, Arimoto Y, Kataoka Y, Shintani T, Morita N, Sugiuchi T, Masuda S, Nakano A, Taiji H, Kaga K. A prevalent founder mutation and genotype–phenotype correlations of *OTOF* in Japanese patients with auditory neuropathy.
Clin Genet 2012: 82: 425–432. © John Wiley & Sons A/S, 2012

Auditory neuropathy is a hearing disorder characterized by normal outer hair cell function and abnormal neural conduction of the auditory pathway. Aetiology and clinical presentation of congenital or early-onset auditory neuropathy are heterogeneous, and their correlations are not well understood. Genetic backgrounds and associated phenotypes of congenital or early-onset auditory neuropathy were investigated by systematically screening a cohort of 23 patients from unrelated Japanese families. Of the 23 patients, 13 (56.5%) had biallelic mutations in *OTOF*, whereas little or no association was detected with *GJB2* or *PJVK*, respectively. Nine different mutations of *OTOF* were detected, and seven of them were novel. p.R1939Q, which was previously reported in one family in the United States, was found in 13 of the 23 patients (56.5%), and a founder effect was determined for this mutation. p.R1939Q homozygotes and compound heterozygotes of p.R1939Q and truncating mutations or a putative splice site mutation presented with stable, and severe-to-profound hearing loss with a flat or gently sloping audiogram, whereas patients who had non-truncating mutations except for p.R1939Q presented with moderate hearing loss with a steeply sloping, gently sloping or flat audiogram, or temperature-sensitive auditory neuropathy. These results support the clinical significance of comprehensive mutation screening for auditory neuropathy.

Conflict of interest

The authors declare no conflict of interest.

T Matsunaga[a], H Mutai[a], S Kunishima[b], K Namba[a], N Morimoto[c], Y Shinjo[d], Y Arimoto[e], Y Kataoka[f], T Shintani[g], N Morita[h], T Sugiuchi[i], S Masuda[j], A Nakano[e], H Taiji[c] and K Kaga[d]

[a]Laboratory of Auditory Disorders, National Institute of Sensory Organs, National Tokyo Medical Center, Tokyo, Japan, [b]Department of Advanced Diagnosis, Clinical Research Center, National Hospital Organization Nagoya Medical Center, Nagoya, Japan, [c]Department of Otorhinolaryngology, National Center for Child Health and Development, Tokyo, Japan, [d]National Institute of Sensory Organs, National Hospital Organization Tokyo Medical Center, Tokyo, Japan, [e]Division of Otorhinolaryngology, Chiba Children's Hospital, Chiba, Japan, [f]Department of Otolaryngology, Head and Neck Surgery, Okayama University Postgraduate School of Medicine, Dentistry and Pharmaceutical Science, Okayama, Japan, [g]Department of Otolaryngology, Sapporo Medical University School of Medicine, Sapporo, Japan, [h]Department of Otolaryngology, Teikyo University School of Medicine, Tokyo, Japan, [i]Department of Otolaryngology, Kanto Rosai Hospital, Kawasaki, Japan, and [j]Department of Otorhinolaryngology, Institute for Clinical Research, National Mie Hospital, Tsu, Japan

Key words: auditory neuropathy – genotype–phenotype correlation – mutation – non-syndromic hearing loss – *OTOF*

Corresponding author: Tatsuo Matsunaga MD, PhD, Laboratory of Auditory Disorders and Department of Otolaryngology, National Institute of Sensory Organs, National Tokyo Medical Center, 2-5-1 Higashigaoka, Meguro, Tokyo 152-8902, Japan.

Tel.:+81 3 3411 0111;
fax:+81 3 3412 9811;
e-mail:
matsunagatatsuo@kankakuki.go.jp

Received 28 February 2012, revised and accepted for publication 6 April 2012

Auditory neuropathy (AN) is a hearing disorder characterized by normal outer hair cell function, as revealed by the presence of otoacoustic emissions (OAE) or cochlear microphonics, and abnormal neural conduction of the auditory pathway, as revealed by the absence or severe abnormality of auditory brainstem responses (ABR) (1). Hearing disorders having the same characteristics have also been reported as auditory nerve disease in adult cases (2). Individuals with AN invariably have difficulties in understanding speech (3), and approximately 10% of infants diagnosed with profound hearing loss have AN (3, 4).

About 50% of subjects with congenital or early-onset AN have risk factors such as perinatal hypoxia, whereas the remaining 50% of subjects are likely to have a genetic factor (3, 5). To date, four loci responsible for non-syndromic AN have been mapped: DFNB9 caused by *OTOF* mutation and DFNB59 caused by *PJVK* mutation, both of which are responsible for autosomal recessive AN; AUNA1 caused by DIAPH3 mutation, which is responsible for autosomal dominant AN; and AUNX1, which is responsible for X-linked AN (6–9). Mutations in *OTOF*, which contains 50 exons and encodes short and long isoforms of otoferlin (10), are the most frequent mutations associated with AN with various frequency depending on the population studied (11–15). Most *OTOF* genotypes have been associated with stable, severe-to-profound hearing loss with only a few exceptions (11–20). Studies of genetic backgrounds and clinical phenotypes in various populations will extend our knowledge of genotype–phenotype correlations and may help in the management and treatment of AN.

Materials and methods

Subjects

We enrolled 23 index patients of unrelated Japanese families with congenital or early-onset AN. Diagnosis of hearing loss was made by age 2 in all patients except for one, who had mild hearing loss diagnosed at age 9. All patients had non-syndromic AN in both ears, and they were collected from all over Japan as part of a multicentre study of AN. Patients with hearing loss of possible environmental risk factors for AN such as neonatal hypoxia or jaundice were excluded. With regard to the family history, one patient had a brother having congenital AN and all others were simplex. DNA samples and medical information were obtained from each proband and, if possible, parents and siblings. For DNA samples, 2 parents, 1 parent, no parent, and 1 sibling were available in 10 families, 4 families, 9 families, and 1 family, respectively. None of parents of 23 index patients complained of hearing loss by clinical interview. For the normal-hearing control, 189 subjects who had normal hearing by pure-tone audiometry were used. This study was approved by the institutional ethics review board at the National Tokyo Medical Center. Written informed consent was obtained from all the subjects included in the study or their parents.

Genetic analysis

DNA was extracted from peripheral blood by standard procedures. Genetic analysis for mutations in *GJB2* and for A1555G and A3243G mitochondrial DNA mutations were conducted in all patients according to published methods (21, 22). Mutation screening of *OTOF* was performed by bidirectional sequencing of amplicons generated by PCR amplification of each exon (exons 1–50) and splice sites using an ABI 3730 Genetic Analyzer (Applied Biosystems, Foster City, CA). Primer sequences for *OTOF* are listed in Table S1, supporting information. Mutation nomenclature is based on genomic DNA sequence (GenBank accession number NG_009937.1), with the A of the translation initiation codon considered as +1. The nucleotide conservation between mammalian species was evaluated by ClustalW (http://www.ebi.ac.uk/Tools/msa/clustalw2/).

To determine whether the prevalent p.R1939Q alleles are derived from a common founder, we conducted haplotype analysis. We genotyped single nucleotide polymorphisms (SNPs) with a minor allele frequency of >0.3 in the Japanese population and a microsatellite marker (D2S2350) spanning the *OTOF* locus and nearby genes on an ABI Genetic Analyzer 310 and Genescan 3.7 software (Applied Biosystems). Forty-four SNPs and the D2S2350 microsatellite marker in the vicinity of the mutation were genotyped in 11 AN patients who had p.R1939Q and in a part of their parents.

In six patients who did not have any mutations in *OTOF* and *GJB2* and three patients who were heterozygous for *OTOF* mutation without any mutations in *GJB2*, all coding exons and splice sites of *PJVK* were sequenced. Primer sequences were designed based on the reference sequence of *PJVK* (GenBank accession number NG_012186) and are listed in Table S2. Novelty of mutations and non-pathogenic variants found in the present study were examined in EVS (http://evs.gs.washington.edu/EVS/) and dbSNP

(http://www.ncbi.nlm.nih.gov/snp). The effect of an amino acid substitution was predicted using PolyPhen-2 software (http://genetics.bwh.harvard.edu/pph2/) and NNSPLICE 0.9 version (Berkley Drosophila Genome Project, http://www.fruitfly.org/seq_tools/splice.html) for the splice sites. The effect of p.D1842N was also analysed by modelling the three-dimensional structure of otoferlin using SWISS-MODEL (http://swissmodel.expasy.org/) (23).

Clinical examination and data analysis

Audiological tests included otoscopic examination and pure-tone audiometry with a diagnostic audiometer in a soundproof room following International Standards Organization standards. On the basis of pure-tone air-conduction thresholds, the degree of hearing loss was determined by the better ear pure-tone average across the frequencies 0.5, 1, 2, and 4 kHz, and it was classified as mild (20–40 dB), moderate (41–70 dB), severe (71–95 dB), or profound (>95 dB) according to the recommendations for the description of audiological data by the Hereditary Hearing Loss Homepage (http://hereditaryhearingloss.org).

Results

Genetic findings

Of 23 patients with a diagnosis of congenital or early-onset AN, 13 (56.5%) carried two pathogenic *OTOF* alleles, and 3 patients (13.0%) carried one pathogenic allele (Fig. 1: inner circle). In summary, ~70% of the patients had pathogenic *OTOF* alleles. Results of genotyping of the detected pathogenic *OTOF* alleles in 13 families carrying two pathogenic *OTOF* alleles (10 families in which two parents were examined and 3 families in which one parent was examined) were compatible with autosomal recessive inheritance in all these families. *OTOF* mutations consisted of three missense mutations, one frameshift mutation, two nonsense mutations, one non-stop mutation, and two putative splice site mutations (Tables 1 and 2). p.R1939Q was previously reported as a mutation and IVS47-2A>G was previously reported in dbSNP. Other seven *OTOF* mutations were novel. p.R1939Q was found in 43.5% of all alleles. We also identified 16 non-pathogenic *OTOF* variants, of which only p.P1697P was novel (Table 1). This variant did not change the score of splice site prediction. The location of each mutation in *OTOF* and the evolutionary conservation of the amino acids or nucleotides affected by the missense and putative splice site mutations are shown in Fig. 2a,b. The frequency of different *OTOF* genotypes is summarized in Fig. 1 (middle circle); 56.5% of the patients had p.R1939Q. In contrast, mutations other than p.R1939Q were confined to individual families. Previously, p.R1939Q was reported in one family with AN in the United States (19), and a different mutation in the same codon (p.R1939W) was reported in another family (16). Screening for the mutation

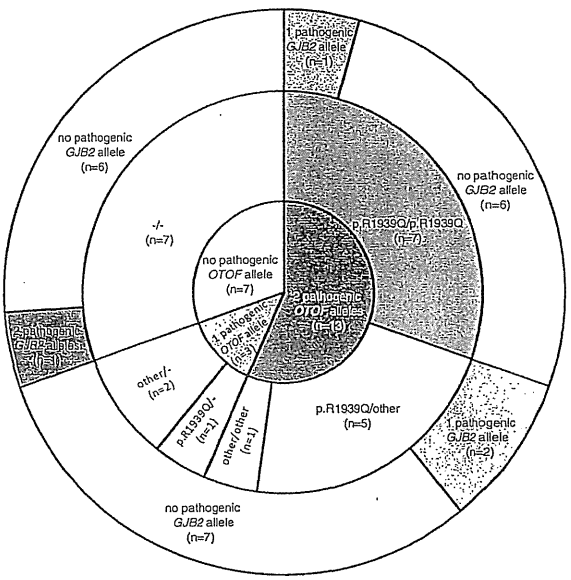

Fig. 1. Genetic backgrounds and frequency of different *OTOF* alleles in patients with congenital or early-onset auditory neuropathy (AN). (a) Distribution of patients carrying different pathogenic *OTOF* alleles (inner circle), *OTOF* genotypes (middle circle), and *GJB2* genotypes (outer circle). p.R1939Q indicates *OTOF* allele with p.R1939Q mutation; other indicates pathogenic *OTOF* alleles except for p.R1939Q allele; *n* indicates number of patients.

in 189 control subjects with normal hearing revealed only one heterozygous carrier. This mutation was predicted to be probably damaging variant according to PolyPhen-2.

The novel missense mutation p.D1842N was identified in a heterozygote without accompanying pathogenic alleles (patient 15). The mutation was predicted to be probably damaging variant according to PolyPhen-2. D1842 is located within the C2F domain, which is one of six calcium-binding modules (C2 domains) in otoferlin that are indispensable for otoferlin function. The predicted three-dimensional protein structure suggested that this mutation generates a repulsive force on calcium ions, resulting in reduced otoferlin activity (Fig. 3a–c). Another novel missense mutation, p.G541S, was identified as homozygous in a patient with parental consanguinity (patient 13). This mutation was predicted to be probably damaging variant according to PolyPhen-2 and involves a change from a non-polar residue to a polar residue in the C2C domain.

The c.1946-1965 del20 frameshift mutation truncates otoferlin at S648, causing a change in stop codon that adds six residues to the C terminus. Two nonsense mutations, p.Y474X and p.Y1822X, also truncate otoferlin. It is possible that these mutations trigger the nonsense-mediated decay response, by which aberrant mRNA is eliminated before translation (24). Even if the truncated proteins were produced, they would not function well because the mutations in c.1946-1965 del20, p.Y474X, and p.Y1822X disrupt three

Table 1. Mutations and non-pathogenic variants in congenital or early-onset auditory neuropathy

Types of variants	Location	Nucleotide variation	Predicted amino acid change	Allele frequency in normal controls	Novel or known
Mutations					
Missense substitution	Exon 15	c.1621G>A	p.G541S	0/376	Novel
	Exon 46	c.5524G>A	p.D1842N	0/376	Novel
	Exon 50	c.5816G>A	p.R1939Q	1/378	Known
Frameshift	Exon 17	c.1946-1965del20	p.R649PfsX5	0/192	Novel
Nonsense	Exon 14	c.1422T>A	p.Y474X	0/192	Novel
	Exon 46	c.5466C>G	p.Y1822X	0/192	Novel
Non-stop substitution	Exon 50	c.5992T>C	p.X1988RextX30	0/192	Novel
Putative splice site mutations					
	Exon 9 IVS	IVS9+5G>A		0/362	Novel
	Exon 47 IVS	IVS47-2A>G		0/190	Known
Non-pathogenic variants					
	Exon 2	c.129C>T	p.D43D	NT	Known
	Exon 3	c.145C>T	p.R49W	3/192	Known
	Exon 3	c.158C>T	p.A53V	75/192	Known
	Exon 4	c.244C>T	p.R82C	29/192	Known
	Exon 5	c.372A>G	p.T124T	NT	Known
	Exon 19	c.62C>T	p.P21L	172/172	Known
	Exon 23	c.2452C>T	p.R818W	0/188	Known
	Exon 24	c.2580C>G	p.V860V	NT	Known
	Exon 24	c.2613C>T	p.L861L	NT	Known
	Exon 25	c.2703G>A	p.S901S	NT	Known
	Exon 25	c.2736G>C	p.L912L	NT	Known
	Exon 41	c.4677G>A	p.V1559V	NT	Known
	Exon 41	c.4767C>T	p.R1589R	NT	Known
	Exon 43	c.5026C>T	p.R1676C	8/188	Known
	Exon 43	c.5091G>A	p.P1697P	NT	Novel
	Exon 45	c.5331C>T	p.D1777D	NT	Known

C2 domains, four C2 domains, and one C2 domain, respectively.

p.X1988RextX30, in which the stop codon is affected and 30 residues are added to the C terminus, accompanied p.R1939Q in a compound heterozygote (patient 12). Because the stop codon is separated by only one residue from the transmembrane domain, the additional C-terminal tail residues would interfere with anchoring to the membrane, which is critical for proper function. The three subjects with only one pathogenic *OTOF* allele (patient 14, patient 15, and patient 16) are likely to have mutations which could not be identified in the present study rather than just be coincidental carriers. Mutations which were not excluded in the present study include those in introns, a previously unknown exon, or a distant enhancer/promotor region as well as large deletions or other sequence rearrangements.

Screening of other genes revealed that one patient who did not have any mutations in *OTOF* was a compound heterozygote of *GJB2* mutations (patient 21). The AN phenotype has been reported in subjects with *GJB2* mutations (25). We identified three other patients with biallelic *OTOF* mutations that had heterozygous *GJB2* mutations, but they were considered to be coincidental. Distribution of patients carrying different pathogenic GJB2 alleles was shown in Fig. 1 (outer circle). None of the patients had A1555G or A3243G mitochondrial DNA mutations. Mutations in *PJVK* were not detected in six patients who did not have any mutations in *OTOF* or *GJB2* as well as in three patients who were heterozygous for *OTOF* mutation without mutations in *GJB2*.

All but one patient had a single haplotype associated with the p.R1939Q variant, which was not represented in 22 wild-type alleles in the parents, and representative SNPs and their allele frequencies as well as haplotypes are shown in Fig. 4a,b. Patient 2 had recombination of the same p.R1939Q-associated haplotype with the wild-type haplotype from his father. These results indicated that all the chromosomes carrying p.R1939Q were derived from a common ancestor.

Clinical findings

Clinical features of the patients are shown in Table 2. A consistent phenotype was present in seven patients carrying homozygous p.R1939Q and four patients who had heterozygous p.R1939Q accompanied by heterozygous truncating or putative splice site mutations. Patient 12, a compound heterozygote of p.R1939Q and a non-truncating mutation, showed a distinct phenoytpe. Patient 13, a homozygote of another non-truncating mutation, presented with temperature-sensitive AN.

Table 2. Genetic and clinical features of patients with congenital or early-onset auditory neuropathy

OTOF genotype[a]	Patient ID	Age, sex	*GJB2* genotype[a]	Degree of hearing loss (age of test)	Phenotype
p.R193Q/p.R1939Q					
	1	3, M	–/–	Profound (1 year 7 months)	NP, flat
	2	2, M	–/–	Profound (2 years 7 months)	NP, flat
	3	3, M	–/–	Profound (3 years 2 months)	NP, flat
	4	4, M	c.235delC/–	Profound (3 years 2 months)	NP, gently sloping
	5	2, F	–/–	profound (2 years 6 months)	NP, gently sloping
	6	2, M	–/–	Severe (2 years 10 months)	NP, flat
	7	2, M	–/–	Severe (1 year 9 months)	NP, flat
p.R1939Q/truncating or putative splice site[b]					
p.R1939Q/c.1946-1965del20	8	9, M	–/–	Unstable (2 years 10 months)	unstable, gently sloping
p.R1939Q/p.Y474X	9	2, M	–/–	Profound (1 year 7 months)	NP, flat
p.R1939Q/p.Y1822X	10	1, F	p.G45E+p.Y136X/–	Profound (2 years 0 month)	NP, flat
p.R1939Q/IVS9+5G>A	11	7, F	–/–	Profound (7 years 6 months)	NP, flat
p.R1939Q/non-truncating[c]					
p.R1939Q/p.X1988RextX30	12	29, F	p.V371/–	Moderate (29 years 1 month)	P, R: steeply sloping L: gently sloping
Non-truncating/non-truncating					
p.G541S/p.G541S	13	26, M	–/–	Mild[d] (25 years 11 months)	NP, flat
Various heterozygotes[e]					
p.R1939Q/–	14	5, F	–/–	Profound (5 years 10 months)	NP, flat
p.D1842N/–	15	2, F	–/–	Moderate (2 years 9 months)	NP, flat
IVS47-2A>G/–	16	6, F	–/–	Profound (5 years 11 months)	NP, flat
No mutations					
	17	4, F	–/–	Severe (4 years 8 months)	NP, gently sloping
	18	7, M	–/–	Profound (7 years 4 months)	NP, gently sloping
	19	6, F	–/–	Severe (5 years 7 months)	NP, R: gently sloping L: flat
	20	8, F	–/–	Profound (8 years 2 months)	NP, gently sloping
	21	3, F	p.235delC/c.176-191del16	Profound (3 years 1 month)	NP, flat
	22	7, F	–/–	Severe (7 years 10 months)	NP, flat
	23	2, M	–/–	Severe (1 year 8 months)	NP, flat

F, female; ID, identification number; M, male; NP, non-progressive; P, progressive; Phenotype (course of hearing loss and audiogram shape).
[a]No mutations.
[b]Truncating or putative splice site mutations.
[c]Non-truncating mutations.
[d]Temperature-sensitive auditory neuropathy.
[e]Mutations in heterozygotes without accompanying pathogenic mutations.

Patient 13 complained of difficulty in understanding conversation, and his hearing deteriorated when he became febrile or was exposed to loud noise according to his self-report. He explained that the deterioration varied from mild to complete loss of communication. Pure-tone audiometry when he was afebrile revealed mild hearing loss with a flat configuration. Among three patients who had only one pathogenic allele of *OTOF*, patient 15 carrying p.D1842N presented with moderate hearing loss, whereas patient 14 carrying p.R1939Q and patient 16 carrying IVS47-2A>G presented with profound hearing loss.

Discussion

The present study demonstrated biallelic *OTOF* mutations in 56.5% (13 of 23) of subjects with congenital or early-onset AN in Japanese population, indicating the most frequent cause associated with this type of AN. So far, biallelic *OTOF* mutations were identified in 22.2% (2 of 9) and 55% (11 of 20) of subjects with AN in American and Spanish studies, respectively (11, 12). In Brazilian population, 27.3% (3 of 11) of subjects with AN had *OTOF* mutations in two alleles (13). Taiwanese and Chinese subjects demonstrated that 18.2% (4 of 22)

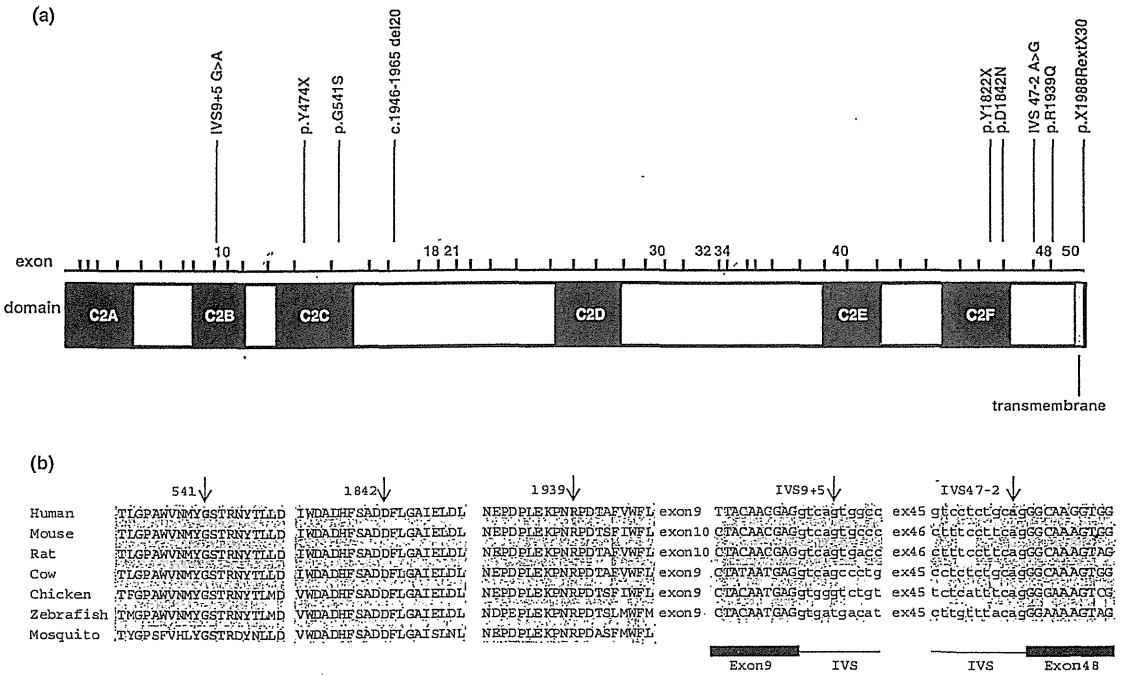

Fig. 2. The location of each mutation in *OTOF* and the evolutionary conservation of the amino acids or nucleotides affected by the missense and splice site mutations. (a) Location of mutations in the *OTOF* coding region of the cochlear isoform. Calcium-binding domains C2A through C2F are shown in black. (b) Multiple alignments of otoferlin orthologs at five non-contiguous regions and splice sites. Arrows indicate affected amino acids or nucleotides. Regions of amino acid and nucleotide sequence identity are shaded. Boundaries between introns and exons are indicated in the bottom. IVS indicates intervening sequence.

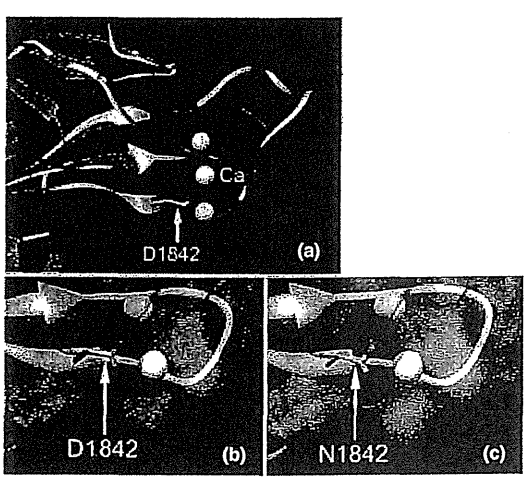

Fig. 3. Predicted three-dimensional protein structures of C2F domain in wild-type otoferlin and D1842N mutant otoferlin. (a) Ribbon model of the otoferlin C2F domain (white) superimposed onto that of the corresponding region of human protein kinase C gamma (hPKCγ, PDBID: 2UZP, chain A) which was selected as an optimal template (29.5% amino acid sequence identity) (magenta). Ca^{2+} is shown as a white sphere. The regions around D1842 of wild-type otoferlin (b) and N1842 of mutant otoferlin (c) are overlaid with their electrostatic surface potentials indicated by red (negative), blue (positive), and white (neutral). The side chains of both D1842 and N1842 are located very close (within 1.0 Å) to calcium ions. D1842N changes the electrostatic surface potential around the side chain from negative to positive in the cellular environment (pH = 7.4), and generate repulsive force on calcium ions.

and 1.4% (1 of 73), respectively, had biallelic *OTOF* mutations (14, 15).

The spectrum of *OTOF* mutations we identified differed significantly from those in other populations. Most reported *OTOF* mutations in the literature have been confined to individual families. An exception is p.Q829X, found in approximately 3% of autosomal recessive non-syndromic sensorineural hearing loss cases in the Spanish population (18). Recently, c.2905-2923delinsCTCCGAGCGCA and p.E1700Q were identified in four Argentinean families and four Taiwanese families, respectively (12, 14). In this study, p.R1939Q was detected in 13 families. Thus, p.R1939Q is now the second-most prevalent *OTOF* mutation reported. This mutation may be more common in Japan, as this mutation is found in only 1 of 10753 choromosomes in the European-American and African-American population by EVS. p.R1939Q was previously reported in one family in the United States, but the origin of the family was not detailed (19). Because no patients carrying p.R1939Q have been reported in Asian population except for the present study or in European population, this prevalent founder mutation appears to be an independent mutational event in Japanese.

Pathogenic *OTOF* mutations have been associated with stable, severe-to-profound sensorineural hearing loss with a few exceptions: c.2093+1G>T and p.P1987R were associated with stable, moderate-to-severe hearing loss (11, 19), p.E1700Q was associated with progressive, moderate-to-profound hearing